Electron scattering at Co(0001) surfaces: Effects of Ti and TiN capping layers

Erik Milosevic and Daniel Gall

Department of Materials Science and Engineering, Rensselaer Polytechnic Institute, 110 8th St, Troy, NY 12180, USA

In situ transport measurements on epitaxial 7.6-nm-thick Co(0001)/Al_2O_3(0001) films with and without Ti and TiN capping layers during O_2 exposure are used to investigate the effects of surface chemistry on electron scattering at Co(0001) surfaces. The Co sheet resistance R_s increases with increasing thickness d_{Ti} and d_{TiN} of the Ti and TiN capping layers, saturating at 8% and 31% above the uncoated Co(0001) for d_{Ti} > 0.2 nm and d_{TiN} > 0.1 nm, respectively. This increase is attributed to electron scattering into local surface states which is less pronounced for Ti than TiN. *In situ* resistance measurements taken during a continuously increasing O_2 partial pressure from 0-40 Pa indicates a relatively steep 24% increase in R_s at an exposure of ~50 Pa·s which can be attributed to Co surface oxidation that leads to atomic level roughness and a decrease in the electron scattering specularity p. Ti and TiN cap layers with $d_{Ti} \geq 0.5$ nm and $d_{TiN} \geq 0.13$ nm exhibit no resistance change upon air exposure, indicating suppression of Co oxidation. These results indicate a promising Co-Ti interface with an electron scattering specularity of p = 0.4-0.5 which is retained during oxygen exposure while, in contrast, electron scattering at the Co-TiN is completely diffuse (p = 0), suggesting that Ti barrier layers facilitate higher-conductivity Co interconnects than TiN barriers, as long as the Ti layer is sufficiently thick ($d_{Ti} \geq 0.5$ nm) to suppress Co oxidation.

I. INTRODUCTION

Electron transport in metallic conductors at the nanometer scale is an area of considerable interest to the semiconductor industry because the resistivity of narrow interconnect wires increases signal delay and power consumption in integrated circuits.[1–4] At wire dimensions near or below the bulk electron mean free path, electron scattering at surfaces,[5–7] grain boundaries,[8–12] and surface roughness[13–15] cause the resistivity to increase well above the bulk value.[16] The resistivity size effect in Co is of particular interest because Co is currently used in the first few metallization levels for the narrowest interconnect lines by multiple integrated circuit manufacturing companies,[17] replacing the previous Cu and W metallization schemes due to a number of advantages, including: (1) a lower melting point in comparison to W, allowing defect healing and grain growth at feasible annealing temperatures,[18] (2) a larger electromigration resistance than for Cu, and (3) thinner and more conductive barrier/adhesion layers,[19] allowing greater volumes of metal fill and lower vertical via resistances.[20]

Electron scattering at surfaces is typically quantified using the classical model by Fuchs and Sondheimer (FS),[21,22] who describe electron-surface interactions phenomenologically using a specularity parameter p that adopts a value between 0 and 1. Zero specularity (p = 0) corresponds to completely diffusive scattering where the electron momentum is randomized upon scattering at the surface, resulting in a resistivity increase. Conversely, specular scattering (p = 1) corresponds to electron reflection from the surface with conservation of the parallel momentum component and, therefore, no effect on the resistivity. Thus, metal surfaces/interfaces that exhibit a large electron scattering specularity are desired for next generation interconnect technologies. Surfaces with partially specular electron scattering have been reported for Ag,[23] Au,[24–26] and Cu,[7,27–29] where the surface of Cu is observed to transition from partially specular with p_1 = 0.6 – 0.7 in vacuum to completely diffuse upon oxidation.[27–29] In addition, studies have revealed that partial

specularity exists at the interfaces between Cu and SiO_2,[30] NiO,[27] TiO_2,[28] AlO_x[31] and TaO_x,[32] indicating that the Cu specularity can be intentionally "tuned" with the proper choice of capping layer. We have recently reported the growth of epitaxial Co(0001) layers and shown that oxygen exposure causes a resistance increase which is attributed to a transition from partially specular (p_1 = 0.55) to diffuse (p_1 = 0) surface scattering upon oxygen exposure,[33,34] similar to the reported effects on Cu(001) surfaces.[7,27–29] These results suggest that the scattering specularity of the Co surface may also be intentionally modulated with appropriate capping layers, which motivates the study presented here.

In this article, we report on the electron scattering at the Co(0001) surface and the effect of surface oxidation and Ti and TiN capping layers on the resistivity. *In situ* transport measurements from nominally 7.6-nm-thick epitaxial Co(0001) layers on c-plane sapphire during O_2 exposure indicate a 24% resistance increase due a surface oxidation that results in a decrease in the electron surface scattering specularity. Ti capping layers suppress the Co oxidation effects and facilitate partially specular electron scattering at the Ti-Co interface. TiN caps also protect Co oxidation but result in in a 55% resistance increase in comparison to bare Co due to a transition to diffuse scattering at the Co-TiN interface, indicating that Ti liners provide a conductivity benefit over TiN liners for Co metallization.

II. PROCEDURE

Co(0001) layers, and Ti and TiN capping layers were deposited in a three-chamber ultra-high vacuum DC magnetron sputtering system with a base pressure of 10^{-7} Pa.[35–37] Polished 10 × 10 × 0.5 mm^3 Al_2O_3(0001) substrates were cleaned ultrasonically in consecutive baths of trichloroethylene, acetone, isopropyl alcohol, and deionized water, mounted to a Mo stub with colloidal silver paint, and inserted into the deposition system through a load lock. Substrates were degassed *in situ* at the Co deposition temperature of 300 °C for one hour. 5-cm-diameter Co (99.95%) and Ti (99.995%) targets were positioned facing the substrate at a 45° tilt and a distance of 9 cm and were sputter-cleaned with closed shutters for 5 min prior to Co depositions which were done in 0.40 ± 0.03 Pa Ar (99.999%) with a continuously rotating substrate. A constant magnetron power of 50 W yielded a deposition rate of 0.10 ± 0.01 nm/s, resulting in a nominal thickness of 7.6 nm for the Co layers deposited for 75 seconds. The films were left at 300 °C for 1 hour after deposition and then allowed to cool to room temperature (295 K) for approximately 12 hours. Subsequently, they were transferred *in situ* to an attached analysis chamber for *in situ* resistance measurements using a linear four-point probe operated at 1-100 mA. The samples were then transferred back to the deposition chamber without air exposure for deposition of either Ti or TiN capping layers at room temperature (295 K) using a ported shutter over the Ti target to limit the deposition rate. Ti caps were deposited at a magnetron power of 100 W in 0.40 Pa Ar yielding a deposition rate of 0.1 nm/min, as determined by X-ray reflectivity analyses. TiN caps were deposited at 100 W in 0.67 Pa N_2 with a deposition rate of 0.03 nm/min. The Ti deposition time was varied from 0 to 1040 seconds to obtain a set of samples with varying effective Ti capping layer thicknesses d_{Ti} = 0 to 2.0 nm. TiN depositions times were varied from 21 to 5536 seconds, yielding nominal cap thicknesses d_{TiN} = 0.0075 to 2.0 nm. The capped Co layers were then moved to the analysis chamber for additional *in situ* transport measurements, including measurements during oxygen exposure. For this purpose, the resistance was continuously measured while introducing a constant flux of a 90%Ar – 10%O_2 gas mixture with the valves to the vacuum pumps closed. This leads to a linearly increasing (0.07 Pa/s) chamber pressure, reaching a 400 Pa total pressure corresponding to a 40 Pa O_2 partial pressure at the end of a ~1.6 h experiment. Finally,

the samples were removed from the system via a load lock and their *ex situ* sheet resistance measured after air exposure using a second four-point probe, as recently reported for epitaxial Nb[38] and Ni[39] layers.

X-ray diffraction (XRD) analyses were performed using a PANalytical X'pert PRO MPD system with a Cu source. ω-2θ survey scans were taken with a divergent beam and a PW3018/00 PIXcel line detector operated in scanning mode. φ-scans were acquired with a point-focus optics using a poly-capillary lens that yields quasi-parallel Cu K_{α} x-rays with a <0.3° divergence, and a 0.27° parallel-plate collimator in front of a scintillation point detector. X-ray reflectivity (XRR) measurements for thickness calibrations were done in the same system, using a parabolic mirror which yields a source divergence of <0.055°, and a scintillation point detector.

III. RESULTS AND DISCUSSION

All Co layers in this study have the same nominal thickness of 7.6 nm and are epitaxial Co(0001) layers as confirmed by XRD methods[5,28,40,41] including ω-2θ and φ scans of the Co 0002 and $10\bar{1}0$ reflections, indicating the epitaxial relationship: Co[0001]$\parallel$$Al_2O_3$[0001] and Co[$10\bar{1}0$]$\parallel$$Al_2O_3$[$11\bar{2}0$] as we have previously reported and described in detail in ref. 33. The Co(0001) films have an average measured *in situ* resistivity of 12.0 ± 1.5 μΩcm, where the stated error bar represents the standard deviation and indicates sample-to-sample variations which are attributed to differences in the effective thickness and crystalline quality. This value is similar to ρ = 12.27 ± 0.64 μΩcm that we have previously reported for 7.9-nm-thick epitaxial Co(0001).[33]

Figure 1 is a plot of the change in sheet resistance ΔR_s caused by the deposition of Ti or TiN cap layers on 7.6-nm-thick Co(0001), plotted as a function of the capping layer thickness d_{cap}. Each data point is determined from one sample and represents the difference between the *in situ* measured R_s before and after deposition of the cap layer. A bare (uncoated) Co film is represented by the data points at d_{cap} = 0 nm where, by definition, there is no sheet resistance change ΔR_s = 0 Ω/□. The resistance of Co films increases when coated with Ti, indicated by an increase in ΔR_s to 0.7 ± 0.6, 1.3 ± 0.9, 1.3 ± 0.1, 0.7 ± 0.2, and 1.4 ± 0.2 Ω/□ for d_{Ti} = 0.13, 0.25, 0.50, 1.0, and 2.0 nm, respectively. This increase is attributed to an increasingly diffuse electron surface scattering caused by the Ti atoms that disturb the electronically smooth Co(0001) surface[29,31] and increase the local surface density of states (LSDOS) at the Fermi level E_f, similar to what has been reported for Al and Ti caps on Cu films.[28,31] That is, the Ti adatoms which develop into a continuous cap layer disturb the flat surface potential and also cause local surface states that electrons scatter into, both causing a decrease in the surface scattering specularity p. This is illustrated with the right y-axis in Fig. 1, which indicates the change in specularity Δp corresponding to the plotted ΔR_s. The Δp is determined using the approximate form of the FS model for distinct top and bottom surfaces,[6] a literature value for the average Co bulk in-plane resistivity ρ_o = 5.6 μΩcm,[42] a room temperature mean free path λ = 19.5 nm,[33] and the nominal Co film thickness of 7.6 nm. We note that all Δp values are negative, indicating a decrease in specularity by 0.07 - 0.14 upon the addition of a Ti cap. This suggests that the Co-vacuum interface specularity, which we have previously reported to be p = 0.55,[33] is reduced to a partial specularity of p = 0.4-0.5 for the Co-Ti interface. This is distinctly different from the previously investigated interfaces of Cu with Ti,[28] Al,[31] and Ta,[7] which all exhibit p = 0 after deposition of a Ti, Al, or Ta cap layer with d_{cap} > 0.16, 1.4, or 0.3 nm, respectively. We attribute the finite scattering specularity of the Co-Ti interface to their similar structure which is also evidenced by their relatively high solubility[43] and is expected to facilitate the epitaxial growth of the thin Ti cap, leading to a smooth coherent interface with partially specular electron scattering, as previously simulated for coated Cu surfaces with smooth and

coherent interfaces.[44,45] Similarly, partially specular scattering has been reported for the coherent Cu-Ni interface,[27] where Cu and Ni also have a similar structure and are miscible.

The plot in Fig. 1 shows that TiN caps on Co(0001) also cause a resistance increase, with ΔR_s = 1.9 ± 0.3, 2.2 ± 0.3, 2.7 ± 0.5, 4.1 ± 0.3, and 5.0 ± 0.2 Ω/□ for d_{TiN} = 0.0075, 0.015, 0.031, 0.063, and 0.13 nm, respectively. This increase up to d_{TiN} = 0.13 nm appears approximately linear on the semi-log plot and suggests a scattering specularity that decreases following approximately an exponential decay, similar to what has been reported for Al on Cu and has been attributed to the increasing LSDOS(E_f) with increasing Al cap thickness.[31] Further increases in d_{TiN} yields no change in ΔR_s = 4.9 ± 0.4, 4.9 ± 0.6, 4.9 ± 0.6, and 4.7 ± 0.2 Ω/□ for d_{TiN} = 0.25, 0.50, 1.0, and 2.0 nm. This ΔR_s corresponds to Δp = -0.51 which nearly matches the magnitude of the reported p = 0.55 for the bare Co surface, suggesting that the TiN deposition causes the Co surface to scatter completely diffuse (p = 0) for $d_{TiN} \geq 0.13$ nm. The decrease in specularity is attributed to the perturbation of the smooth Co(0001) surface and the development of local surface states, which is the same argument as for the Ti caps. However, the final resistance and specularity are quite different for the Ti and TiN caps, with p = 0.4-0.5 for the Co-Ti interface but p = 0 for the Co-TiN interface.

Fig. 2 shows representative curves indicating the change in sheet resistance ΔR_s during *in situ* exposure to an increasing O_2 partial pressure, from nominally 7.6-nm-thick epitaxial Co(0001) with Ti and TiN caps. The x-axis indicates the total oxygen exposure Φ_{O2} over five orders of magnitude, from 0.5 to 10^5 Pa·s. The black curve in Fig. 2(a) is from the uncoated Co sample, showing a continuous resistance increase with increasing Φ_{O2}. ΔR_s increases approximately logarithmically up to ΔR_s = 0.40 Ω/□ at Φ_{O2} = 10 Pa·s, followed by a steep increase to 1.90 Ω/□ between 10 and 50 Pa·s, and a more gradual increase to ΔR_s = 2.61 Ω/□ at the end of the experiment with $\Phi_{O2} = 1\times10^5$ Pa·s. The overall shape of this curve is distinctly different from what has previously been reported from a similar experiment with Cu(001), which shows a peak in ΔR_s at 1.3 Pa·s that is attributed to the adsorption of a partial molecular oxygen monolayer and a steep increase between 2×10^3 and 2×10^4 Pa·s due to chemical oxidation of the Cu surface.[31] Similarly, we attribute the rapid resistance increase shown in Fig. 2 for Co to chemical surface oxidation which, however, occurs at an exposure Φ_{O2} = 10-50 Pa·s that is approximately two orders of magnitudes smaller than for Cu and is likely associated with the higher reactivity of Co and the associated lower (more negative) oxide formation enthalpy.[46] Correspondingly, the monolayer adsorption peak and valley cannot be observed for Co because of the early onset of the resistance increase due to chemical oxidation which dominates over the resistance decrease expected for the formation of an adsorbed oxygen monolayer. The blue curve in Fig. 2(a) from a Co layer coated with 0.13 nm Ti exhibits a constant ΔR_s for Φ_{O2} < 4 Pa·s, a small local maximum of 0.08 Ω/□ at 7 Pa·s, and a minimum of -0.05 Ω/□ at 27 Pa·s followed by a rapid increase between 30 and 600 Pa·s to a final ΔR_s = 2.73 Ω/□ at $\Phi_{O2} = 1\times10^5$ Pa·s. The steep increase is attributed to chemical oxidation of the Co surface which is initially suppressed by oxidation of the more reactive Ti and therefore occurs at nearly an order of magnitude higher Φ_{O2} than for the pristine Co sample. This shift of the Co chemical oxidation to a larger exposure allows observation of a clear but small peak and valley in ΔR_s at 7 and 27 Pa·s which are attributed to the perturbation of the surface potential by a partial and then complete adsorbed oxygen monolayer on both the Ti cap as well as fractions of the Co surface that are not covered with Ti adatoms, qualitatively matching what has previously been reported for Cu(001).[29,31] We note that the negative ΔR_s is not only facilitated by a smooth surface potential of the adsorbed oxygen but also by chemical oxidation of the Ti which converts from a metal to a dielectric, reducing the LSDOS at E_f and promoting more specular scattering at

the Co surface, similar to what has been shown for Ti deposited on Cu.[28] The green curve from the d_{Ti} = 0.25 nm sample is qualitatively identical to the d_{Ti} = 0.13 nm curve. However, the increase due to Co oxidation is delayed by another two orders of magnitude to 10^4-10^5 Pa·s and the region with a negative ΔR_s is much more pronounced, showing a minimum ΔR_s = -0.26 Ω/□ at 700 Pa·s. Both of these effects are attributed to the greater effective thickness and corresponding surface coverage of the d_{Ti} = 0.25 nm sample. More specifically, the additional Ti increases the time for oxidation and therefore delays Co oxidation. It also results in a larger coverage of Co by dielectric TiO_2 which facilitates specular scattering at the Co surface and therefore a negative ΔR_s. The red curve in Fig. 2(a) from a Co sample capped with 2.0 nm Ti shows a ΔR_s that remains nearly constant over the entire exposure range. The absence of an increase in ΔR_s indicates a negligible Co-oxidation effect, which is attributed to the 2-nm-thick Ti forming a continuous and protective layer on the Co. The slight dip at 12 Pa·s may be associated with oxygen adsorption which temporarily smoothens atomic level roughness of the Ti surface while the gentle decrease around 10^4 Pa·s is an experimental artifact due to a slight decrease in sample temperature after Ti deposition, as confirmed with reference samples.

Fig. 2(b) is the corresponding plot for the resistance change during oxygen exposure of Co layers coated with TiN caps. The black line is the curve from the uncoated Co sample which is already shown in Fig. 2(a) but is replicated here to facilitate easier comparison. The dark-blue line is from a sample with a d_{TiN} = 0.015 nm thick TiN cap layer, corresponding to just 7% of a TiN monolayer. It is qualitatively similar to the bare Co curve, showing a continuous increase in ΔR_s with the steepest slope (in this semi-log plot) at around Φ_{O2} = 10 Pa·s. This value is comparable to the 10-50 Pa·s range for the bare Co, indicating that the steep increase is attributed to oxidation of the Co surface that is not covered by the 7% monolayer TiN cap. Overall, this sample shows a slower resistance increase than the bare Co sample, indicating that even 7% of a TiN monolayer provides some oxidation protection. However, at large exposures, ΔR_s continues to increase to reach 3.35 Ω/□ at 1×10^5 Pa·s which is larger than for the bare Co sample. This difference may be due to experimental variations but may also indicate that a surface with oxidized TiN causes more diffuse electron scattering than a bare oxidized Co surface, similar to the d_{Ti} = 0.13 nm curve in Fig. 2(a) which is slightly above the d_{Ti} = 0 nm curve for large Φ_{O2}. The dark-green curve in Fig. 2(b) from a sample with a 0.13 nm TiN cap shows only a small increase in ΔR_s to 0.50 Ω/□ at Φ_{O2} = 10^5 Pa·s, indicating that even this approximately 0.6 monolayer coating already provides substantial oxidation protection. This protection becomes complete for larger d_{TiN}, as indicated by the dark red line in Fig 2(b) for d_{TiN} = 1.0 nm which shows negligible variations in ΔR_s except for a slight decrease due to the same temperature effect as discussed above for the d_{Ti} = 2.0 nm sample.

Fig. 3(a) shows the change in sheet resistance ΔR_s due to oxygen exposure of 7.6-nm-thick Co(0001) films with Ti or TiN cap layers vs their cap thickness. Each data point is obtained from one specific sample by taking the difference in the sheet resistance measured after removal from the vacuum system minus that measured *in situ* after cap layer deposition but prior to O_2 exposure. Here, the O_2 exposure includes both the *in situ* exposure to a 90%Ar – 10%O_2 gas mixture with increasing pressure to 400 Pa as well as the exposure to atmospheric pressure air for approximately 10 min, yielding a total O_2 exposure of ~10^7 Pa·s. The first data point at d_{cap} = 0 nm indicates the resistance change ΔR_s = 3.29 ± 0.23 Ω/□ due to oxidation of the bare Co layer. This value is larger than the ΔR_s = 2.61 Ω/□ for Φ_{O2} = 1×10^5 Pa·s presented in Fig. 2 for the same sample, indicating that the resistance of the bare Co sample continues to increase as the sample is exposed to atmospheric pressure air. We note, however, that a fraction of this difference may also be due to experimental uncertainty of ± 0.2 Ω/□ since the *in situ* and *ex situ* sheet resistances are measured

with two distinct experimental setups. The positive ΔR_s is attributed to the chemical oxidation of the Co surface, as mentioned above, resulting in (1) atomic-scale roughening of the conductive Co which causes diffuse electron scattering and (2) consumption of some metallic Co by the developing oxide layer, effectively reducing the conductive cross-sectional area.[31] In order to quantitatively determine the magnitude of the second effect, we measure the Co oxide thickness by XRR and determine the loss of metallic Co to the oxide as we have previously described in Ref. 33. This analysis indicates that the majority (50-80%) of the resistance increase can be attributed to the loss of metallic Co and that the measured ΔR_s corresponds to a change in resistivity $\Delta\rho$ = 0.84 μΩcm with a corresponding change in the surface scattering specularity Δp = -0.1. This specularity decrease is smaller than the Δp = -0.55 that we have previously reported for the Co(0001) surface oxidation in air. We do not know the exact cause for this difference but speculate that the controlled low-pressure oxidation in the argon-oxygen mixture may result in a smoother (less defect containing) metal-oxide interface than during a (humid) air exposure, leading to partially specular scattering at the interface between Co and Co-oxide in this study. We note that the measured Δp has a relatively large experimental uncertainty due to the time delay between transport measurements and the oxide quantification by XRR and also note that no systematic difference in the interface between the Co film and its oxide could be detected by XRR between dry-O_2 and air exposed samples, which both exhibit root-mean-square roughnesses of 0.3-0.4 nm.

The Co film coated with 0.13 nm of Ti yields a ΔR_s = 3.61 ± 0.75 Ω/□ which, within uncertainty, is equal to that of bare Co, confirming that the partial coverage of d_{Ti} = 0.13 nm is not sufficient to inhibit Co oxidation. ΔR_s decreases to 1.87 ± 0.70 Ω/□ for d_{Ti} = 0.25 nm, indicating partial oxidation protection by the Ti cap, and drops to approximately zero for d_{Ti} = 0.50, 1.0, and 2.0 nm with measured values of ΔR_s = -0.20 ± 0.18, -0.18 ± 0.20, and -0.12 ± 0.30 Ω/□. Thus, Ti capping layers with $d_{Ti} \geq 0.5$ nm completely suppress the resistance increase associated with Co oxidation, indicating that these caps are likely continuous layers. We note that these ΔR_s values are even slightly negative, suggesting that the Ti-oxidation may result in a Co-TiO_2 metal-dielectric interface which facilitates specular electron scattering. This interpretation is consistent with previous reports on a resistance decrease during oxidation of Cu layers that were coated with 0.4 nm of Al[31] or 0.6 nm of Ti.[28]

Fig. 3(a) also shows the measured ΔR_s for Co coated with TiN. It is 4.46 ± 0.35, 3.95 ± 0.27, 4.51 ± 0.38, and 3.15 ± 0.29 Ω/□ for d_{TiN} = 0.0075, 0.015, 0.031, and 0.063 nm, corresponding to an average ΔR_s = 4.02 Ω/□ in this thickness range. This is 22% larger than ΔR_s = 3.29 Ω/□ for bare Co, suggesting that sub-0.1-nm-thick TiN capping layers may exacerbate the roughening and/or the specularity loss at the Co surface upon oxidation. The plotted ΔR_s drops to approximately zero for $d_{TiN} \geq 0.13$ nm with measured ΔR_s = 0.26 ± 0.24, 0.32 ± 0.42, 0.34 ± 0.76, and 0.11 ± 0.99 Ω/□ for d_{TiN} = 0.13, 0.25, 0.50, and 1.0. That is, TiN forms a protective capping layer even if its nominal thickness is only 0.13 nm, which is below ~0.2 nm for a TiN monolayer. This may be attributed to an overstoichiometric N-to-Ti ratio in the Ti cap such that the excess adsorbed surface nitrogen[47,48] blocks Co oxidation.

Figure 3(b) is a similar plot of the change in sheet resistance vs cap layer thickness. However, contrary to Fig. 3(a), the plotted ΔR_s includes here the resistance change due to both cap layer deposition and oxygen exposure. That is, the data points represent the difference between the resistance measured after air exposure minus the *in situ* R_s prior to the deposition of a cap layer. Thus, they correspond to the sum of the values plotted in Figs. 1 and 3(a). The data point for the bare Co sample (d_{cap} = 0 nm) is identical to that shown in Fig. 3(a), since the pre-cap and post-cap R_s are identical in the absence of a capping layer. In contrast, d_{Ti} = 0.13 and 0.25 nm result in larger

ΔR_s values than in Fig. 3(a), because the deposition of the Ti cap causes a resistance increase prior to oxygen exposure. Larger Ti cap thicknesses result in a relatively small $\Delta R_s \sim 1\ \Omega/\square$ for $d_{Ti} \geq 0.5$ nm. This is due to the effective suppression of Co oxidation by the Ti layer such that the ΔR_s approximately matches the values in Fig. 1. The data for the Co films coated with TiN cap layers qualitatively resemble those for the Ti coatings. They show the largest ΔR_s for small $d_{TiN} \leq 0.063$ nm and a drop to an approximately constant $\Delta R_s \sim 5\ \Omega/\square$ for $d_{TiN} \geq 0.13$ nm which is attributed to suppression of Co oxidation. However, the 5 $\Omega/\square$ for the TiN caps is considerably larger than the 1 $\Omega/\square$ for the Ti caps, which is attributed to the larger reduction in scattering specularity for the TiN vs the Ti coatings, as discussed above and shown in Fig. 1. This suggests that Ti is the more promising barrier material than TiN for Co-metallization, if considering only the resistivity benefit.

IV. CONCLUSIONS

7.6-nm-thick epitaxial Co(0001) samples were sputter deposited onto c-plane sapphire substrates and coated *in situ* with either Ti or TiN capping layers with thicknesses ranging from 0 to 2.0 nm. The change in sheet resistance resulting from oxidation of the Co(0001) surface and/or the capping layers was measured in real-time using *in situ* measurements performed as a function of oxygen exposure. The uncoated Co surface readily oxidizes upon O_2 exposure, leading to a resistance increase that this attributed to a drop in the electron surface scattering specularity and an effective decrease in the film thickness due to Co consumption by the developing surface oxide. Ti cap layers with $d_{Ti} \geq 0.5$ nm protect the Co from oxidation and promote a relatively high conductance which is attributed to partially specular (p = 0.4 - 0.5) electron scattering at the Co-Ti interface which does not decrease upon oxygen exposure. TiN cap layers also protect Co from oxidation, even for very thin d_{TiN} = 0.13 nm layers. However, the resistance is considerably higher than for the Ti caps, which is attributed to completely diffuse electron scattering at the Co-TiN interface. Consequently, Ti represents the more promising liner/barrier material then TiN for low resistance Co interconnects, as long as the Ti barrier is thick enough ($d_{Ti} \geq 0.5$ nm for our processing conditions) to suppress Co oxidation.

ACKNOWLEDGMENTS

The authors acknowledge funding from SRC under tasks 2966 and 2881, the NY State Empire State Development's Division of Science, Technology and Innovation (NYSTAR) through Focus Center-NY–RPI Contract C150117, and the NSF under grant No. 1740271 and 1712752.

References

[1] J. Kelly, J.H.-C. Chen, H. Huang, C.K. Hu, E. Liniger, R. Patlolla, B. Peethala, P. Adusumilli, H. Shobha, T. Nogami, T. Spooner, E. Huang, D. Edelstein, D. Canaperi, V. Kamineni, F. Mont, and S. Siddiqui, in *2016 IEEE Int. Interconnect Technol. Conf. / Adv. Met. Conf.* (IEEE, 2016), pp. 40–42.
[2] J.S. Chawla, S.H. Sung, S.A. Bojarski, C.T. Carver, M. Chandhok, R. V. Chebiam, J.S. Clarke, M. Harmes, C.J. Jezewski, M.J. Kobrinski, B.J. Krist, M. Mayeh, R. Turkot, and H.J. Yoo, in *2016 IEEE Int. Interconnect Technol. Conf. / Adv. Met. Conf.* (IEEE, 2016), pp. 63–65.
[3] N.A. Lanzillo, H. Dixit, E. Milosevic, C. Niu, A. V Carr, P. Oldiges, M. V Raymond, J. Cho, T.E. Standaert, and V.K. Kamineni, J. Appl. Phys. **123**, 154303 (2018).
[4] D. Gall, in *2018 IEEE Int. Interconnect Technol. Conf.* (IEEE, 2018), pp. 157–159.
[5] E. Milosevic, S. Kerdsongpanya, A. Zangiabadi, K. Barmak, K.R. Coffey, and D. Gall, J. Appl. Phys. **124**, 165105 (2018).
[6] J.S. Chawla, F. Gstrein, K.P. O'Brien, J.S. Clarke, and D. Gall, Phys. Rev. B **84**, 235423 (2011).
[7] J.S. Chawla and D. Gall, Appl. Phys. Lett. **94**, 252101 (2009).
[8] M. César, D. Gall, and H. Guo, Phys. Rev. Appl. **5**, 054018 (2016).
[9] M. César, D. Liu, D. Gall, and H. Guo, Phys. Rev. Appl. **2**, 044007 (2014).
[10] K. Barmak, A. Darbal, K.J. Ganesh, P.J. Ferreira, J.M. Rickman, T. Sun, B. Yao, A.P. Warren, and K.R. Coffey, J. Vac. Sci. Technol. A Vacuum, Surfaces, Film. **32**, 061503 (2014).
[11] T.-H. Kim, X.-G. Zhang, D.M. Nicholson, B.M. Evans, N.S. Kulkarni, B. Radhakrishnan, E.A. Kenik, and A.-P. Li, Nano Lett. **10**, 3096 (2010).
[12] J.M. Rickman and K. Barmak, J. Appl. Phys. **114**, 133703 (2013).
[13] P.Y. Zheng, T. Zhou, B.J. Engler, J.S. Chawla, R. Hull, and D. Gall, J. Appl. Phys. **122**, 095304 (2017).
[14] Y. Ke, F. Zahid, V. Timoshevskii, K. Xia, D. Gall, and H. Guo, Phys. Rev. B **79**, 155406 (2009).
[15] T. Zhou, P. Zheng, S.C. Pandey, R. Sundararaman, and D. Gall, J. Appl. Phys. **123**, 155107 (2018).
[16] D. Gall, J. Appl. Phys. **127**, (2020).
[17] A. Yeoh, A. Madhavan, N. Kybert, S. Anand, J. Shin, M. Asoro, S. Samarajeewa, J. Steigerwald, C. Ganpule, M. Buehler, A. Tripathi, V. Souw, M. Haran, S. Nigam, V. Chikarmane, P. Yashar, T. Mule, Y. Wu, K. Lee, M. Aykol, K. Marla, P. Sinha, S. Kirby, H. Hiramatsu, W. Han, M. Mori, M. Sharma, H. Jeedigunta, M. Sprinkle, C. Pelto, M. Tanniru, G. Leatherman, K. Fischer, I. Post, and C. Auth, in *2018 IEEE Int. Interconnect Technol. Conf.* (IEEE, 2018), pp. 144–147.
[18] V. Kamineni, M. Raymond, S. Siddiqui, F. Mont, S. Tsai, C. Niu, A. Labonte, C. Labelle, S. Fan, B. Peethala, P. Adusumilli, R. Patlolla, D. Priyadarshini, Y. Mignot, A. Carr, S. Pancharatnam, J. Shearer, C. Surisetty, J. Arnold, D. Canaperi, B. Haran, H. Jagannathan, F. Chafik, and B. L'Herron, in *2016 IEEE Int. Interconnect Technol. Conf. / Adv. Met. Conf.* (IEEE, 2016), pp. 105–107.
[19] S. Dutta, S. Beyne, A. Gupta, S. Kundu, S. Van Elshocht, H. Bender, G. Jamieson, W. Vandervorst, J. Bommels, C.J. Wilson, Z. Tokei, and C. Adelmann, IEEE Electron Device Lett. **39**, 731 (2018).
[20] C. Auth, A. Aliyarukunju, M. Asoro, D. Bergstrom, V. Bhagwat, J. Birdsall, N. Bisnik, M. Buehler, V. Chikarmane, G. Ding, Q. Fu, H. Gomez, W. Han, D. Hanken, M. Haran, M. Hattendorf, R. Heussner, H. Hiramatsu, B. Ho, S. Jaloviar, I. Jin, S. Joshi, S. Kirby, S. Kosaraju, H. Kothari, G. Leatherman, K. Lee, J. Leib, A. Madhavan, K. Marla, H. Meyer, T. Mule, C. Parker, S. Parthasarathy, C. Pelto, L. Pipes, I. Post, M. Prince, A. Rahman, S. Rajamani, A. Saha, J.D. Santos, M. Sharma, V. Sharma, J. Shin, P. Sinha, P. Smith, M. Sprinkle, A.S. Amour, C. Staus, R. Suri, D. Towner, A. Tripathi, A. Tura, C. Ward, and A. Yeoh, in *2017 IEEE Int. Electron Devices Meet.* (IEEE, 2017), pp. 29.1.1-29.1.4.
[21] K. Fuchs and N.F. Mott, Math. Proc. Cambridge Philos. Soc. **34**, 100 (1938).
[22] E.H. Sondheimer, Adv. Phys. **1**, 1 (1952).
[23] J.S. Chawla and D. Gall, J. Appl. Phys. **111**, 043708 (2012).
[24] G. Kästle, H.-G. Boyen, A. Schröder, A. Plettl, and P. Ziemann, Phys. Rev. B **70**, 165414 (2004).
[25] M.S.P. Lucas, Thin Solid Films **2**, 337 (1968).
[26] J.R. Sambles, K.C. Elsom, and D.J. Jarvis, Philos. Trans. R. Soc. A Math. Phys. Eng. Sci. **304**, 365 (1982).
[27] P.Y. Zheng, R.P. Deng, and D. Gall, Appl. Phys. Lett. **105**, 131603 (2014).
[28] P. Zheng, T. Zhou, and D. Gall, Semicond. Sci. Technol. **31**, 055005 (2016).
[29] J.S. Chawla, F. Zahid, H. Guo, and D. Gall, Appl. Phys. Lett. **97**, 132106 (2010).
[30] T. Sun, B. Yao, A.P. Warren, K. Barmak, M.F. Toney, R.E. Peale, and K.R. Coffey, Phys. Rev. B **79**, 041402 (2009).
[31] E. Milosevic and D. Gall, IEEE Trans. Electron Devices **66**, 2692 (2019).
[32] S.M. Rossnagel and T.S. Kuan, J. Vac. Sci. Technol. B Microelectron. Nanom. Struct. **22**, 240 (2004).

[33] E. Milosevic, S. Kerdsongpanya, M.E. McGahay, A. Zangiabadi, K. Barmak, and D. Gall, J. Appl. Phys. **125**, 245105 (2019).
[34] E. Milosevic, S. Kerdsongpanya, and D. Gall, in *2018 IEEE Nanotechnol. Symp.* (IEEE, 2018), pp. 1–5.
[35] B. Wang, S. Kerdsongpanya, M.E. McGahay, E. Milosevic, P. Patsalas, and D. Gall, J. Vac. Sci. Technol. A **36**, 061501 (2018).
[36] B. Wang and D. Gall, Thin Solid Films **688**, 137165 (2019).
[37] M.E. McGahay and D. Gall, Appl. Phys. Lett. **114**, 131602 (2019).
[38] E. Milosevic, S. Kerdsongpanya, M.E. McGahay, B. Wang, and D. Gall, IEEE Trans. Electron Devices **66**, 3473 (2019).
[39] E. Milosevic, P. Zheng, and D. Gall, IEEE Trans. Electron Devices **66**, 4326 (2019).
[40] R. Deng, B.D. Ozsdolay, P.Y. Zheng, S. V. Khare, and D. Gall, Phys. Rev. B **91**, 045104 (2015).
[41] P. Zheng, B.D. Ozsdolay, and D. Gall, J. Vac. Sci. Technol. A Vacuum, Surfaces, Film. **33**, 061505 (2015).
[42] H. Masumoto, H. Saito, and M. Kikuchi, Sci. Reports Res. Institutes Tohoku Univ. Ser. A-Physics Chem. Metall. **S 18**, 84 (1966).
[43] G. Cacciamani, R. Ferro, I. Ansara, and N. Dupin, Intermetallics **8**, 213 (2000).
[44] V. Timoshevskii, Y. Ke, H. Guo, and D. Gall, J. Appl. Phys. **103**, 113705 (2008).
[45] F. Zahid, Y. Ke, D. Gall, and H. Guo, Phys. Rev. B **81**, 045406 (2010).
[46] W.F. Kieffer, J. Chem. Educ. **27**, 659 (1950).
[47] M.A. Wall, D.G. Cahill, I. Petrov, D. Gall, and J.E. Greene, Surf. Sci. **581**, L122 (2005).
[48] M.A. Wall, D.G. Cahill, I. Petrov, D. Gall, and J.E. Greene, Phys. Rev. B **70**, 035413 (2004).

Figures

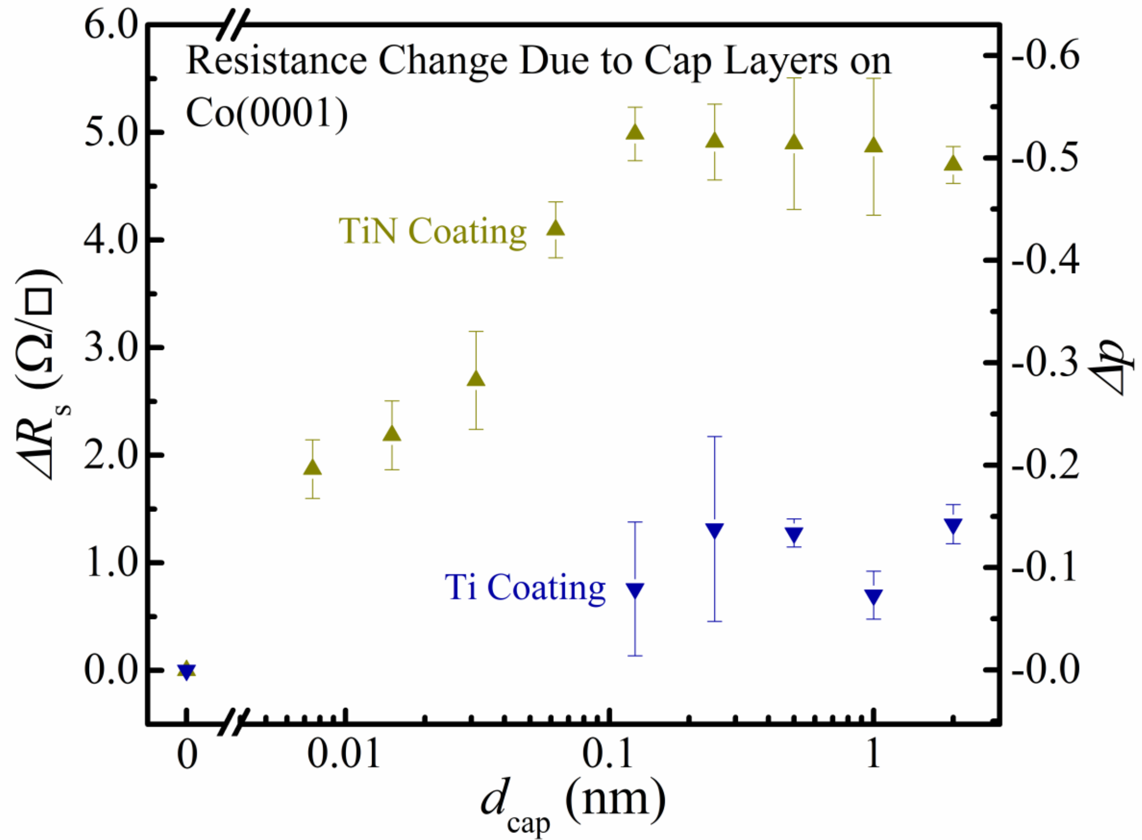

FIG. 1. Change in *in situ* sheet resistance ΔR_s due to Ti (dark blue) and TiN (yellow) cap layers with thickness d_{cap} on top of nominally 7.6-nm-thick Co(0001) films grown on c-plane sapphire. The right axis indicates the corresponding change in the electron surface scattering specularity Δp.

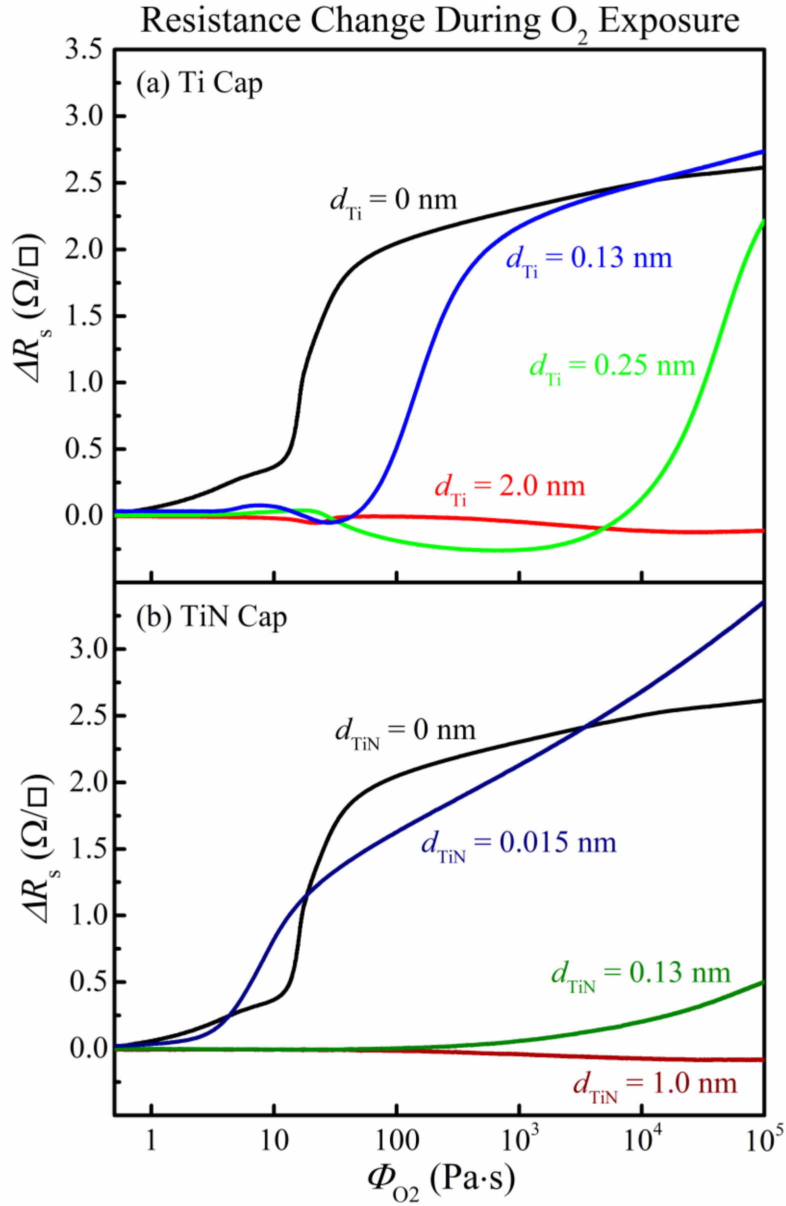

FIG. 2. Change in *in situ* sheet resistance ΔR_s as a function of oxygen exposure from 0.5 to 10^5 Pa·s for Co(0001) coated with (a) Ti cap layers with thickness d_{Ti} = 0, 0.13, 0.25, 2.0 nm, and (b) TiN cap layers with thickness d_{TiN} = 0, 0.015, 0.13, 1.0 nm. The black curve from bare Co without cap layer is duplicated in (a) and (b).

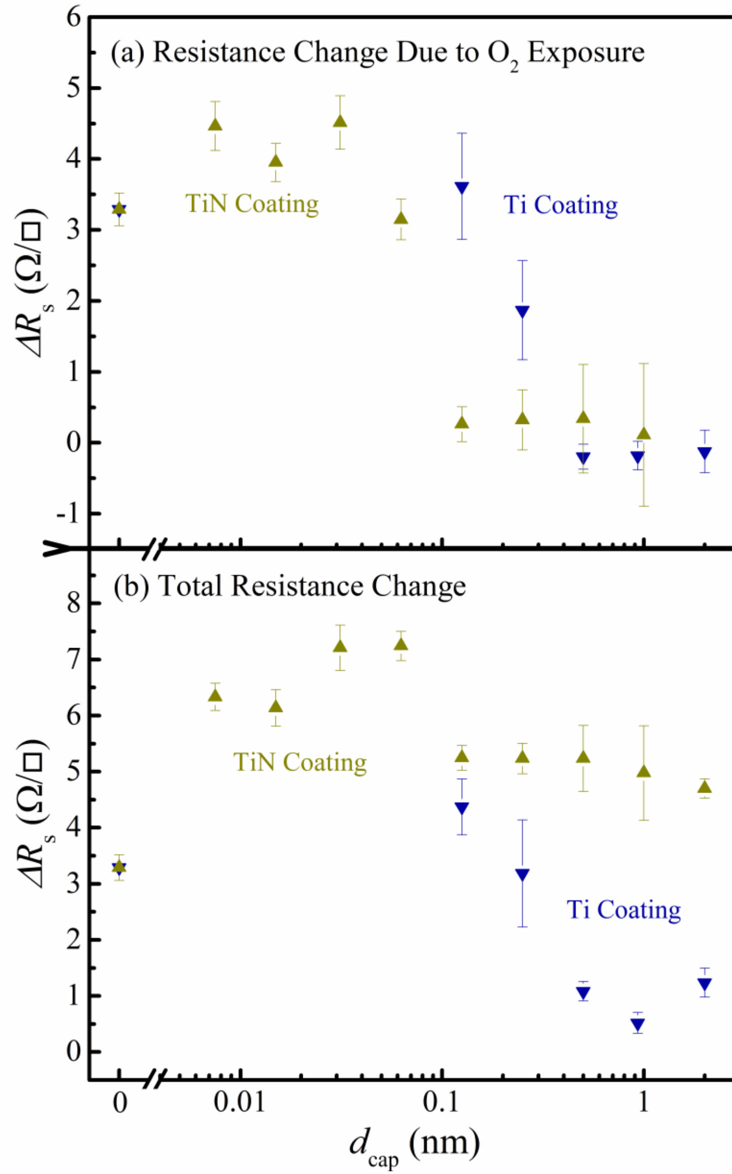

FIG. 3. Change in sheet resistance ΔR_s due to (a) oxygen exposure and (b) capping and surface oxidation of nominally 7.6-nm-thick Co(0001) films coated with Ti (dark blue) and TiN (yellow) as a function of cap layer thickness d_{cap}.